



Crustal architecture of the Transantarctic Mountains between the Scott and Reedy Glacier region and South Pole from aerogeophysical data

Michael Studinger ^{a,*}, Robin E. Bell ^a, Paul G. Fitzgerald ^b, W. Roger Buck ^a

^a *Lamont-Doherty Earth Observatory of Columbia University, Palisades, NY 10964, United States*

^b *Department of Earth Sciences, Syracuse University, Syracuse, NY 13244, United States*

Received 7 April 2006; received in revised form 11 July 2006; accepted 18 July 2006

Editor: C.P. Jaupart

Abstract

Aerogeophysical data collected in transects between the South Pole and West Antarctica, crossing the Transantarctic Mountains at the 150°W meridian, are used to constrain the sub-ice topography, the sub-ice geology and the inland structure of the Transantarctic Mountains. Forward modeling of gravity data suggests slight **crustal thickening of 5 km** beneath the mountain front indicating partial isostatic compensation by thickened crust. New magnetic data help characterize the sub-ice geology inland of the Transantarctic Mountains with the observed magnetic anomaly field **dominated by Granite Harbour Intrusives**, similar to the magnetic field in Victoria Land. However, the typical pattern of anomalies caused by Jurassic tholeiitic magmatism elsewhere along the Transantarctic Mountains is not observed, nor is the mesa topography that is often associated with the Ferrar Dolerite. Together, these observations **rule out the widespread presence of Ferrar Dolerite sills** within the survey area. A pronounced magnetic lineament, herein named the **South Pole Lineament**, parallel to the 0°/180° longitudinal meridian, beneath the South Pole defines a previously unknown tectonic trend of the East Antarctic craton. The lineament suggests the presence of a lithospheric-scale structure beneath South Pole, projecting into a fault mapped from ice-penetrating radar data and extending to Shackleton Glacier, the site of a major geological boundary across the Transantarctic Mountains. Potentially, the lineament is the expression of the edge of the undeformed craton, an inherited structure created during assembly or breakup of Rodinia and Gondwana supercontinents; or an intracontinental transform.

© 2006 Elsevier B.V. All rights reserved.

Keywords: Antarctica; Transantarctic Mountains; Aerogeophysics; Gravity; Magnetism; Radar echo sounding

1. Introduction

The Transantarctic Mountains bisect the Antarctic continent and define a lithospheric and morphologic boundary between East and West Antarctica [1] (Fig. 1).

The Transantarctic Mountains have experienced repeated orogenies, since Rodinia assembly during the Proterozoic and Early Paleozoic followed by Rodinia breakup, and the transition from a passive to an active subducting margin during Gondwana assembly (the Ross Orogeny) [2]. Active margin activity ceased along the Transantarctic Mountains at ~ 480 Ma, followed by 10–15 km of erosion to form the Kukri Peneplain [3], on

* Corresponding author. Tel.: +1 845 365 8598; fax: +1 845 365 8179.
E-mail address: mstudying@ldeo.columbia.edu (M. Studinger).

which shallow marine and alluvial plain sediments of the Beacon Supergroup were deposited from the Devonian to Triassic. In the Mid-Jurassic, intrusion and extrusion of tholeiitic magmas along the Transantarctic Mountains marks the initial breakup of Gondwana [e.g., 4 5 6].

The Transantarctic Mountains and associated West Antarctic rift system are among the most enigmatic tectonic regions on Earth and the mechanism of their formation remain controversial or poorly understood. Most tectonic models for the formation of the present-day Transantarctic Mountains assume they were formed (i.e., uplifted) simultaneously with rifting in the Ross Embayment, and that much of the uplift was related to Early Eocene rifting along the East Antarctic side of the West Antarctic rift system [e.g., 7, and references

herein]. Difficulties in resolving the formation of the Transantarctic Mountains arise from 1) a poor understanding of the age and distribution of basins within the West Antarctic rift system, largely due to the ice cover of the Ross Ice Shelf and the West Antarctic Ice Sheet, 2) the uncertain nature of the boundary between the West Antarctic rift system and the Transantarctic Mountains, including crustal expressions and contrasts in the mantle structure, 3) the gap in the geologic record between the extrusion of Jurassic tholeiitic magmatism (Ferrar Dolerite and Kirkpatrick Basalt, ~ 180 Ma) and the latest Eocene glacial sediments (~ 34 Ma) cored in the Ross Embayment [7–9], 4) a lack of delineation of the inland structure of the Transantarctic Mountains, and 5) poor knowledge of the crustal thickness under the Transantarctic Mountains and cratonic East Antarctica.

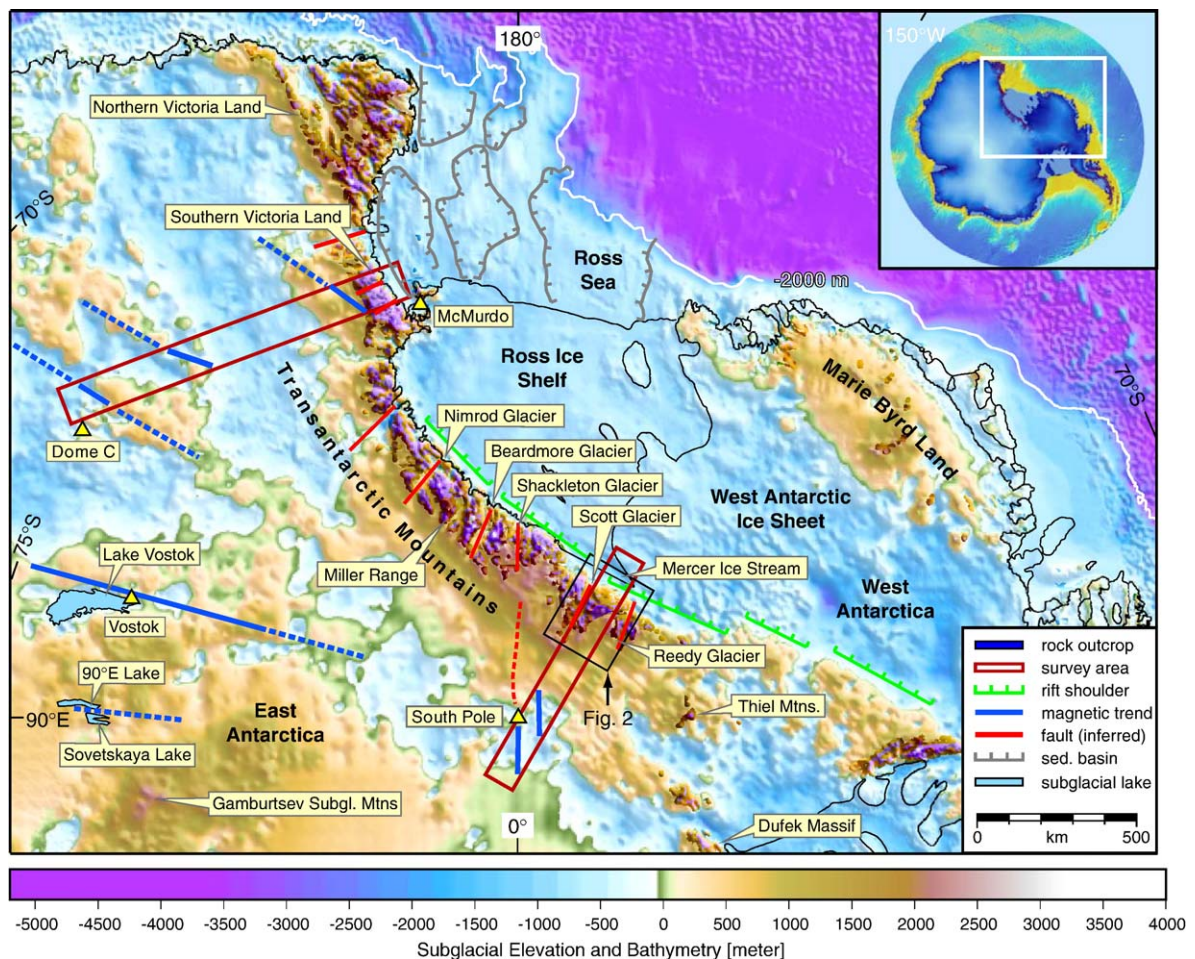


Fig. 1. Subglacial topography and bathymetry of Antarctica [60]. The West Antarctic rift system is the entire area of intracontinental extension defined by the region under the Ross Sea, the Ross Ice Shelf, and the West Antarctic Ice Sheet. The transect from Dome C to McMurdo in southern Victoria Land is discussed in Studinger et al. [10]. The transect between South Pole and Mercer Ice Stream (formerly Ice Stream A) is described here. Dashed fault line is proposed fault by Drewry [28] between the South Pole and the Transantarctic Mountains.

In order to better understand the tectonic and geologic framework, geophysical remote sensing of the hinterland is a crucial step forward.

The goal of this paper is to better constrain the subice morphology, geology, and crustal structure of the southern Transantarctic Mountains from aerogeophysical data. We present evidence for an important tectonic boundary oriented at a high angle to the trend of the Transantarctic Mountains, and document variations in crustal architecture along the mountains that become evident through comparison of two aerogeophysical transects oriented perpendicular to the trend of the Transantarctic Mountains (Fig. 1). The northern transect extends from Dome C to McMurdo and has previously been described in Studinger et al. [10]. The southern transect, described here, ranges from South Pole towards Mercer Ice Stream (formerly Ice Stream A) and covers an area of 810×100 km (Fig. 1).

2. Geology of the survey area

The basement rocks of the Scott Glacier–Reedy Glacier region comprise Proterozoic and Early Paleozoic metasediments and a vast Cambro-Ordovician granitic batholith [11] (Fig. 2). The Proterozoic La Gorce Formation [12] is a folded sequence of metagraywacke and metapelites that was intruded by the Wyatt Formation, a silicic porphyry with hypabyssal and extrusive phases [12,13]. Clastic rocks with interbedded volcanics of the Ackerman Formation conformably overlie the Wyatt Formation in the La Gorce Mountains [14]. Metamorphic rocks along the front of the Transantarctic Mountains, notably in the Harold Byrd Mountains, comprise pelitic and calc-silicate schists, bimodal volcanics, quartzites and marbles with rare Cambrian fossils belonging to the Leverett and Party Formations (these formations do not

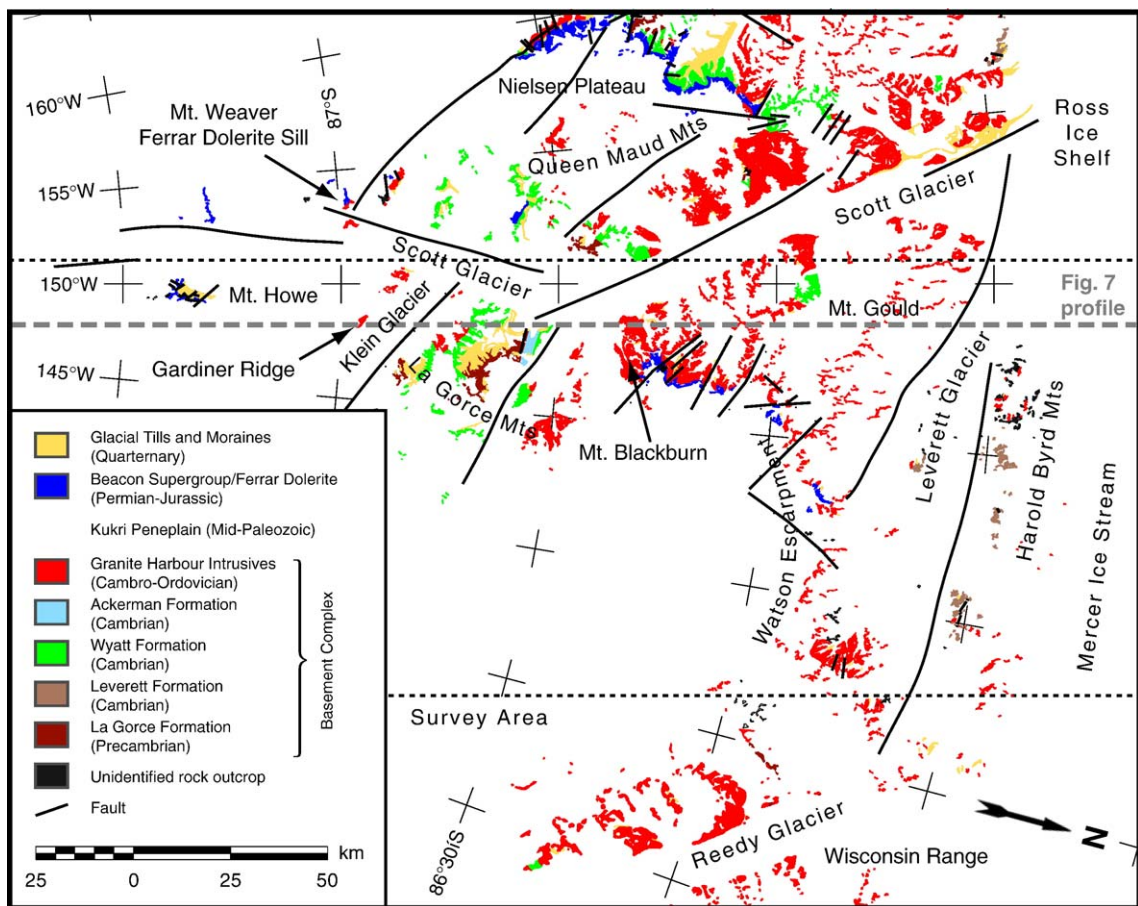


Fig. 2. Simplified geologic map of survey area between the Transantarctic Mountains front and the southernmost rock outcrops. Basemap is based on a compilation by Davis and Blankenship [61 and references herein]. Locations of known faults are from [19] and [21]. Location of magnetic profile in Fig. 7 is indicated by gray dashed line. For location of map area see Fig. 1.

appear in Fig. 2 due to their limited extent) [11,12,15]. During the Cambro-Ordovician Ross Orogeny, deformation of existing rocks and voluminous calc-alkaline magmatism, represented by the Queen Maud-Wisconsin Range batholith of the Granite Harbour Intrusives, resulted from active plate margin processes along the length of the Transantarctic Mountains [11,16–18]. Following the Ross Orogeny, basement rocks were eroded to form the Kukri Peneplain, upon which glacial,

shallow marine and alluvial plain sediments of the Beacon Supergroup were deposited from the Permian to Triassic. Sills of Jurassic Ferrar Dolerite intrude basement rocks and Beacon strata. The geomorphic expression of the Transantarctic Mountains in this region is a dissected mountain front with high plateaus inland, capped by flat-lying strata of the Beacon Supergroup at high elevations in the Mt. Blackburn region and on the west side of the Scott Glacier (Fig. 2).

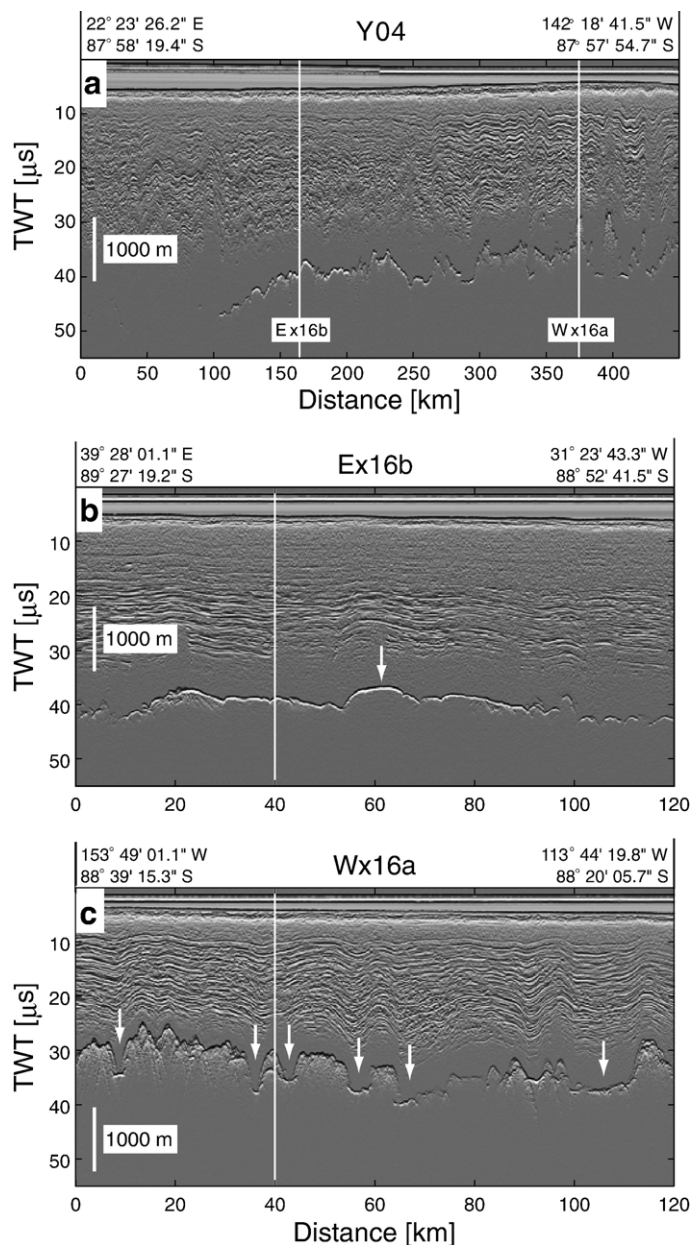


Fig. 3. Ice-penetrating radar profiles. For location of profiles see Fig. 5c. TWT is two-way travel time in μs . Locations of cross lines are indicated by solid white lines. White arrows mark topographic features discussed in the text.

The dramatic Watson Escarpment typifies the transition from the plateaus to the mountain front. Within our survey area, the Kukri Peneplain varies in elevation from 2200 m to 3700 m and is exposed from the La Gorce Mountains, through Mount Blackburn to the Watson Escarpment (Fig. 2).

Katz [19] mapped faults from field observations and aerial photography and inferred several faults from lineaments along major outlet glaciers, as well as using the elevation of the Kukri Peneplain to compile a structural map of the base of the Beacon Supergroup. Because of the proximity of our survey area to the geographic South Pole and the resulting extreme longitudinal convergence, we have rotated all orientations into the reference longitude of the Prime Meridian (0° longitude) using Siddoway and Siddoway's conversion¹ [20]. In addition, commonly used orientations relative to site specific geographic north are given in brackets. Faults in the survey area as mapped or inferred by Katz [19] are primarily oriented 165° (135°W). These near-vertical normal faults reflect post-Beacon deformation of the region into a series of horst and graben structures. The vertical throw is generally of the order of a few hundred meters. Fitzgerald and Stump [21] used offset apatite fission track age profiles to extend Katz's [19] map of post-Beacon faulting to the front of the Transantarctic Mountains on the west side of Scott Glacier. They interpreted the age of faulting as Cenozoic since faults offset Cenozoic fission track ages [21]. Although the timing of the faulting is only weakly constrained, the structural deformation of the Kukri Peneplain and Beacon Supergroup is difficult to reconcile with a regional upwarping model for the formation of the Transantarctic Mountains as proposed for southern Victoria Land [e.g., 22]. Furthermore, the observed denudation pattern does not reveal the exponential regional upwarping required by flexural unloading of a broken plate [21].

3. Aerogeophysical data

3.1. Survey design

In ice covered regions, aerogeophysical imaging is the optimum approach to survey large areas and to resolve geological structures and topography beneath the ice. Aeromagnetic and gravity data are often used in

conjunction with the sub-ice morphology to document the regional tectonic fabric. Aeromagnetic data delineate variations in magnetic rocks in the crust and regional positive anomalies often reflect magnetite-bearing batholiths, large volumes of volcanic rocks, and metamorphic rocks derived from mafic igneous protoliths [e.g., 23]. Magnetic lows can be caused by weakly magnetized rocks, such as sediments or reversely magnetized volcanic rocks. Gravity data reflect the differences of densities between subsurface rocks. The observed variations in the gravity data can be used to interpret geologic structures such as sedimentary basins or granite plutons causing often gravity lows. On a regional scale, gravity data are often used to infer mechanisms of isostatic compensation and crustal thickness variations.

Aerogeophysical data consisting of gravity, magnetics and ice-penetrating radar were simultaneously collected onboard a ski-equipped DHC-6 Twin Otter aircraft by the National Science Foundation's Support Office for Aerogeophysical Research (SOAR) during the 1998/1999 field season. The survey was flown on a grid with 11 flight lines spaced 10 km apart and a total of 28 tie lines spaced 30 km apart; an acquisition of more than 13,000 line-km of aerogeophysical data. The survey was flown at constant barometric altitudes. Flight elevations were 3400 m with occasional departures due to weather conditions or elevated terrain. Several segments of the flight lines over the northernmost 90 km over Mercer Ice Stream were flown at 800 m. Most of the data acquisition and reduction parameters are identical with the southern Victoria Land transect [10].

3.2. Positioning

Positioning of the aircraft was achieved by simultaneously collecting dual-frequency carrier phases of the Global Positioning System (GPS) at a 1-Hz-rate by three receivers on the aircraft and three receivers at the base station. A differential carrier phase solution has been calculated for each flight using the Kinematic and Rapid Static (KARS) GPS package [24].

3.3. Ice-penetrating radar

The SOAR ice-penetrating radar system operated at a frequency of 60 MHz with a pulse width of 250 ns and a repetition interval of 80 μ s [25]. 2048 subsequent

¹ To convert a site specific orientation to a specified reference frame (here 0° longitude) Siddoway and Siddoway [20] used a transformation similar to the Antarctic Navigational Grid: $S_C = \text{MOD}[(S_M + \Delta L), 360]$ where S_C =converted orientation; S_M =site specific measured orientation; ΔL =angle in degrees longitude between the reference site and the study site (for our case ΔL =longitude of the study site); and 360=the divisor.

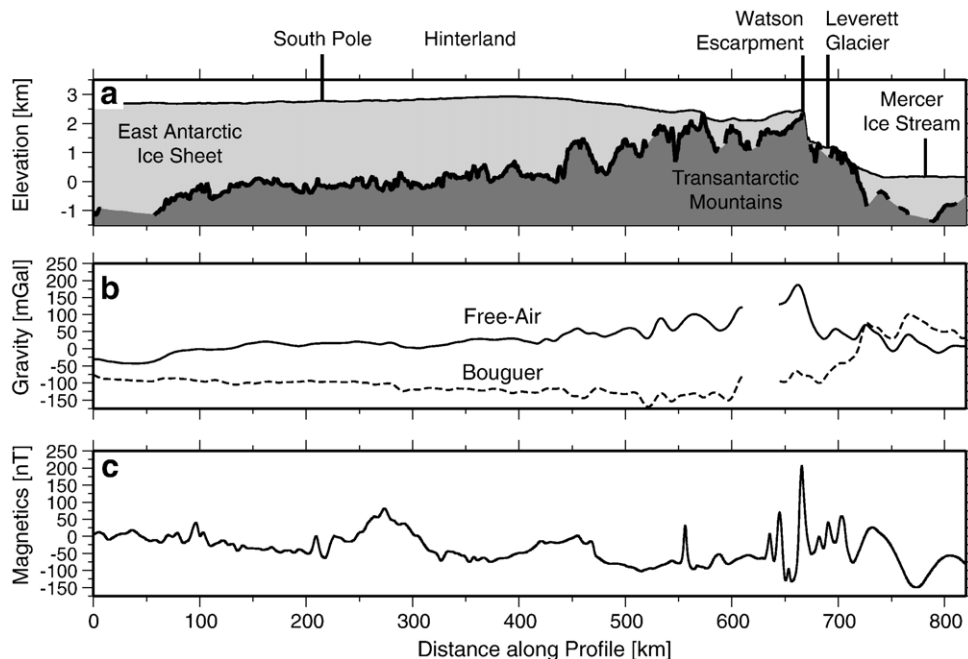


Fig. 4. Transect along the survey area showing a) topography, b) gravity, and c) magnetics. The profile is located in the center of the survey area. Projection of South Pole is denoted. Heavy black lines between ice and bedrock in a) mark areas where the ice thickness was determined from radar reflections at the bed.

records are stacked to yield a single data trace. The ice-penetrating radar data were geo-referenced to the WGS-84 ellipsoid. Subglacial topography was calculated using the ice and rock surface reflections of the ice-penetrating radar and the ice thickness measurements. The standard deviation of the crossover errors at line intersections is 17 m for the surface elevation estimates and 54 m for the ice thickness estimates.

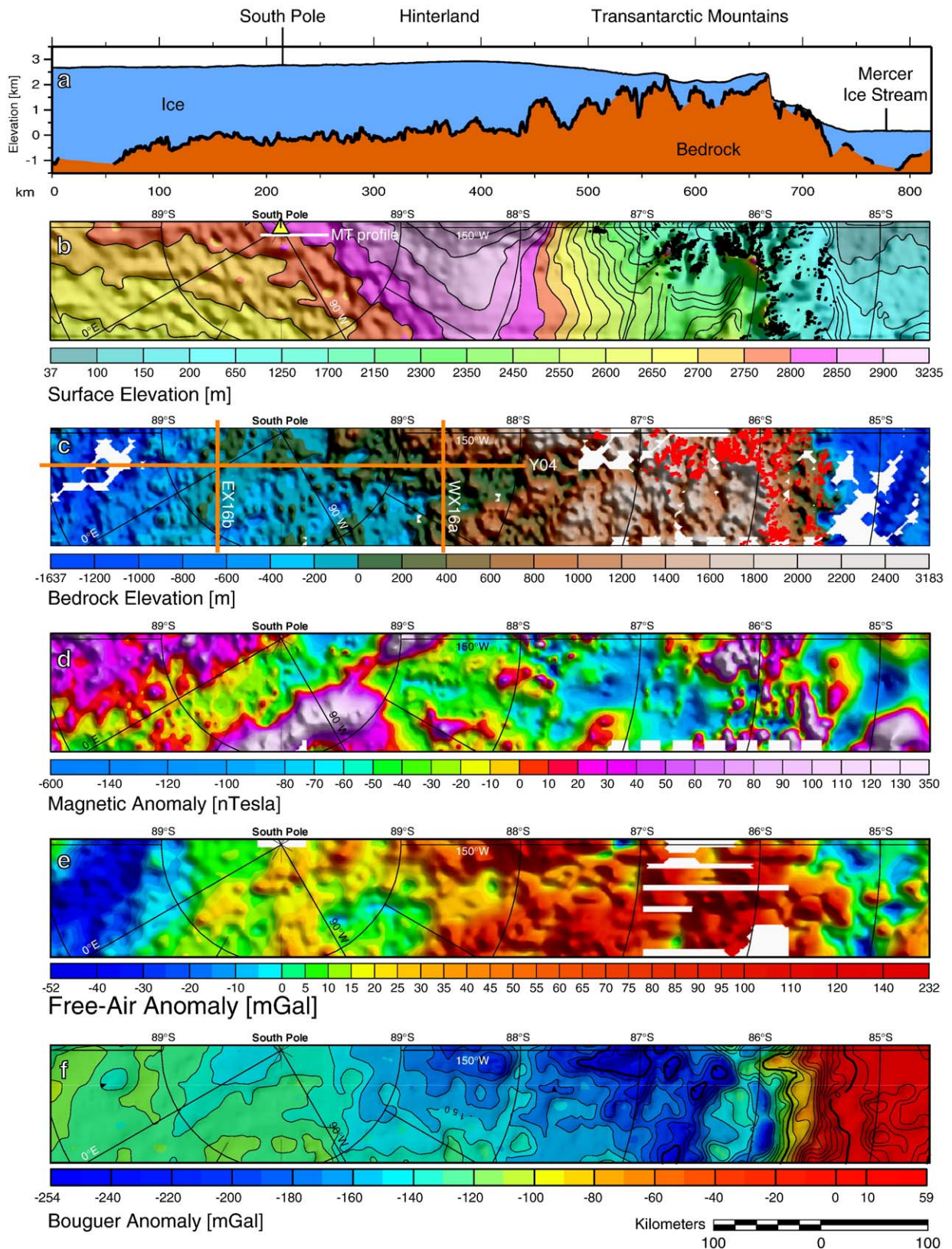
3.4. Magnetics

The total intensity of the Earth's magnetic field was recorded by a towed Cesium vapor magnetometer. Differences in flight elevations were compensated for by two-dimensional upward or downward continuation of the profiles to 3400 m. A trend of order two was removed from the profiles in order to improve the internal consistency of the magnetic data. The standard deviation of the network adjusted crossover error is 20 nT.

3.5. Gravity

The gravity field was measured using a Bell Aerospace BGM-3 gravimeter. High-amplitude noise was removed from the raw gravity data using a low-pass filter in the frequency domain. The filter is a cosine taper that begins its roll-off at 0 Hz and reaches infinite attenuation at 0.006 Hz [26,27]. Differences in flight elevations were compensated for by respective 2-D upward or downward continuation of the profiles to 3400 m. Crossover errors at intersections between flight lines and tie lines have been minimized by linear trend removal. The standard deviation of the network adjusted crossover error is 6.2 mGal and represents the accuracy of the aerogravity data. In addition, the uncertainty of the aerogravity data has been estimated from repeat flights of the same profile. More than 800 line-km were reflown in the southern part of the survey near South Pole. The standard deviation of the differences between the repeat flights is 5.1 mGal.

Fig. 5. (a) Cross-section along the survey area and distance scale for orientation. (b) Ice and rock surface elevation from ice-penetrating radar in meters above sea level. Black areas mark rock outcrops. Contour lines are 50 m apart except for regions with high relief and steep topography where the number of contour lines are reduced. Magnetotelluric profile (MT) is from Wannamaker et al. [56]. Triangle at South Pole marks seismic soundings [54,55]. (c) Bedrock elevation in meters above sea level. Rock outcrops are marked in red. Location of ice-penetrating radar profiles of Fig. 3 are marked. (d) Total field magnetic anomaly in nT at 3400 m elevation. (e) Free-air anomaly in mGal at 3400 m elevation. (f) Bouguer anomaly in mGal at sea level. Contour interval is 10 mGal except for regions with steep gradients.



We have used the gridded free-air gravity and ice surface and subglacial topography data to compute a Bouguer anomaly in the frequency domain [10], using bulk densities of 900 kg m^{-3} and 2670 kg m^{-3} for ice and bedrock, respectively.

4. Topography, gravity and magnetic anomalies

4.1. Subglacial topography

Between the South Pole and the apex of the Transantarctic Mountains, the subglacial topography displays considerable variation, most likely due to a combination of different lithologies, the presence of structures such as faults, or erosional modification of the landscape perhaps accentuated by differential erosion of lithologies such as sandstone and dolerite sills (Figs. 3–5). The sub-ice rock elevation near the South Pole is close to sea level, then generally increases with increasing roughness and greater relief to more than 3000 m at the mountain front where rocks are exposed along the Watson Escarpment. There is a dramatic reduction in bedrock elevation from the Watson Escarpment to the base of the Mercer Ice Stream, where sub-ice elevations are more than 1000 m below sea level (Figs. 4a,5c). Along the 150°W meridian the elevated topography of the Transantarctic Mountains is wider ($>250 \text{ km}$) than anywhere else along the mountain range, except for northern Victoria Land, where accreted terranes are present outboard of the more classic Transantarctic Mountains stratigraphy that typically consists of metasedimentary and granitic basement rocks unconformably overlain by sediments of the Beacon Supergroup and intruded by sills of the Jurassic Ferrar Dolerite (Fig. 1). Four distinct provinces can be defined within the survey area [e.g., 28,29]: 1) a low lying region beneath South Pole with smooth topography and generally bright bed reflections, 2) a region with deeply incised U-shaped valleys on the inland flank of the Transantarctic Mountains, 3) the Transantarctic Mountains with exposed rock outcrops and considerable relief, and 4) the low lying region beneath Mercer Ice Stream and the Ross Ice Shelf.

The subglacial topography at the interior end of the survey rectangle near South Pole shows a depression less than 100 km wide where radar returns from the bedrock are mostly absent (Figs. 3a, 4a, 5c). The topographic minimum is adjacent to a region of smooth topography near South Pole (km 0–250 in Fig. 3a), previously interpreted as an interior lowland [28]. The significance of this topographic feature remains to be determined. Relief on the cross profile Ex16b (Fig. 3b) is a few hundred meters with wavelengths of tens of

kilometers (marked by arrow). The topographic smoothness could result from deposition of clastic material possibly derived from the Transantarctic Mountains or from glacial smoothing, such as commonly occurs under continental ice sheets.

Inboard of the exposed Transantarctic Mountains the sub-ice surface is much rougher, with deeply incised U-shaped valleys, separated by small plateaus (Fig. 3c, marked by arrows). Drewry [28] referred to this zone as upland plains and upland tableland, with the steep U-shaped valleys indicative of glacial erosion. The high reflectivity of the valley floors may be caused by glacial deposits. Between $88^\circ30' \text{ S}$ and 87°S , the subglacial morphology changes from topography dominated by U-shaped valleys to dissected mountains with exposed outcrops and high elevations (Fig. 5). Within our survey area no mesa landscape, such as observed along the inland flank of the Transantarctic Mountains inboard of southern Victoria Land [10,30], is readily distinguishable. Within the Transantarctic Mountains and along their hinterland, such mesa or terraced topography often exists where resistant dolerite sills have intruded flat-lying Beacon Supergroup strata. However, as is discussed below, exposed Ferrar Dolerite sills are noticeably absent from the region between the Scott and Reedy Glaciers and hence by inference from the geophysical data, they are also largely absent inland from this region.

Between 86°S and $85^\circ30' \text{ S}$, high relief and a steep slope in the topography marks the mountain front and the transition towards the Mercer Ice Stream and Ross Ice Shelf with low lying and smooth topography.

4.2. Magnetism

The total field magnetic anomaly can be divided into four segments based on the wavelength, trends and amplitudes of the anomalies. The segments, similar to those defined for subglacial topography, are the South Pole area, the hinterland of the Transantarctic Mountains, the Transantarctic Mountains, and the Ross Ice Shelf/Mercer Ice Stream area. These four segments are shown in: 1) a representative profile (Fig. 4c), 2) the map of the entire survey area (Fig. 5d), and 3) a section of the survey over the Transantarctic Mountains Front in the region with rock outcrops (Fig. 6).

The most obvious structure within the magnetic data is a 60-km-wide linear low parallel to the Prime Meridian at South Pole (Fig. 5d). Within this magnetic low, amplitudes decrease from 0 nT near the edge of the survey area facing East Antarctica (near 15°W and $88^\circ30' \text{ S}$) to -60 nT near the edge of the survey area facing the Transantarctic Mountains (near 150°W and $89^\circ30' \text{ S}$). This low trends

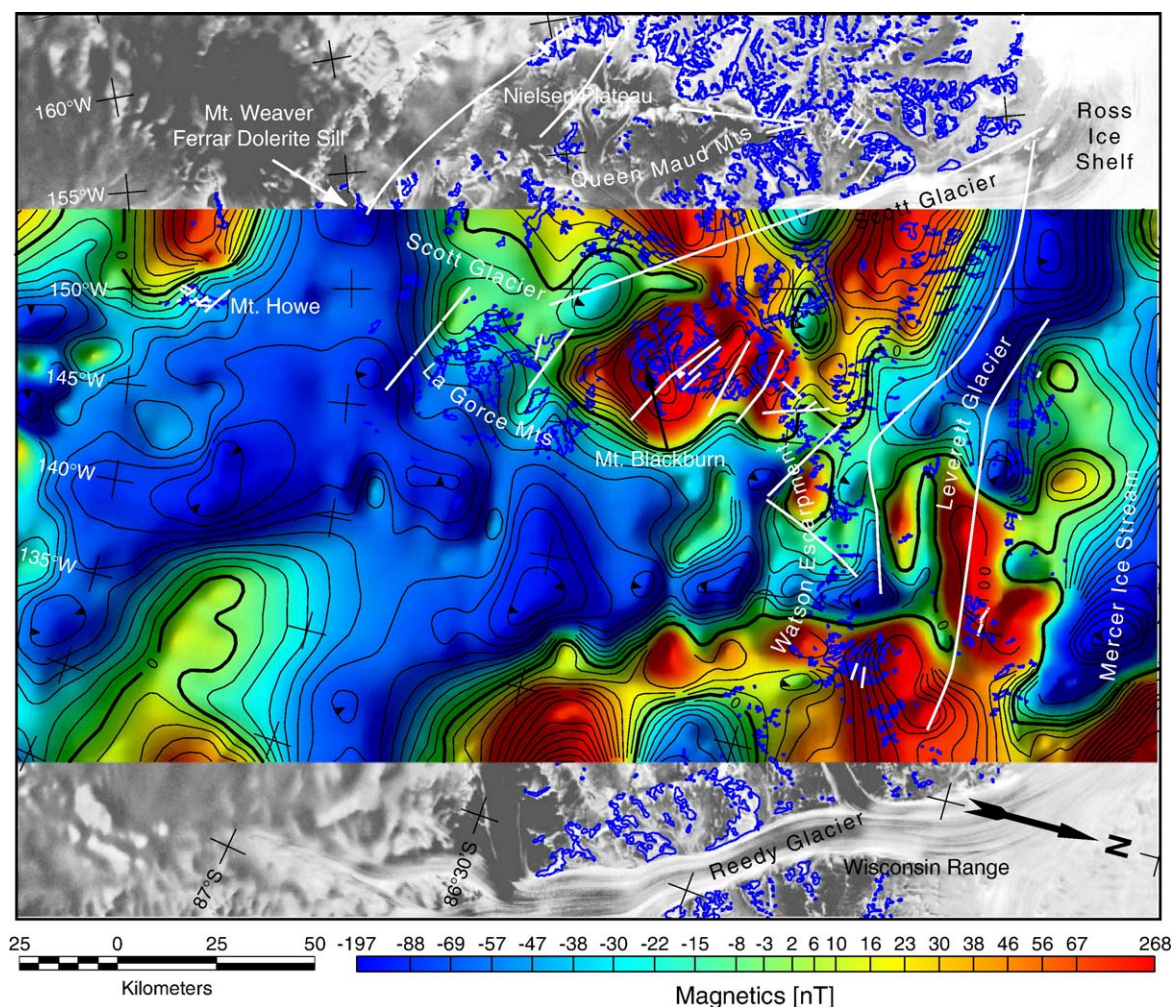


Fig. 6. Portion of the magnetic anomaly map between the Transantarctic Mountains front and the southern boundary of rock outcrops (blue). Contour lines are 10 nT except for areas with steep gradient where the number of contour lines are reduced. Locations of known faults (solid white lines) are from [19] and [21]. Rock outcrops are outlined in blue. Basemap is RADARSAT mosaic [62].

180° (0°), and is remarkably linear for more than 250 km. The magnetic low is flanked on its East Antarctic side by a plateau with positive amplitudes between 20 and 50 nT, and occasional circular shaped anomalies of more than 100 nT and 10–30 km diameter. The edge of this plateau, or flank of the magnetic low, coincides with the location of South Pole. On the Transantarctic Mountain side, the magnetic low is flanked by a positive linear anomaly, between 30 and 60 km wide, with amplitudes greater than 150 nT. This positive anomaly narrows to 20 km near South Pole at 120°W. The magnetic low and its flanks are not associated with a topographic expression (Fig. 5c) or a gravity signature (Fig. 5f).

The magnetic field over the hinterland between South Pole and the Transantarctic Mountains (87°30'S to 88°30'S) shows several apparently circular shaped positive and

negative anomalies. The width of these anomalies is 10–30 km, often only defined by 2 to 3 flight lines (Fig. 5d). The positive anomalies reach up to 100 nT on profile data. Some of the negative anomalies (near 88°S and 150°W) reach amplitudes of –760 nT on profile data with peak-to-trough amplitudes of up to 900 nT (Fig. 5d). The distance between flight elevation and bedrock is about 2000 m over these highly negative anomalies suggesting **highly magnetic reversely magnetized source rocks**. Within the region between 87°30'S and 88°30'S, where a series of oval-shaped magnetic anomalies occur, we can discern no clear structural trend, although we note that the line spacing of 10 km is insufficient to define possible trends within this smaller region.

Over the Transantarctic Mountains, the magnetic anomaly pattern is dominated by shorter wavelengths

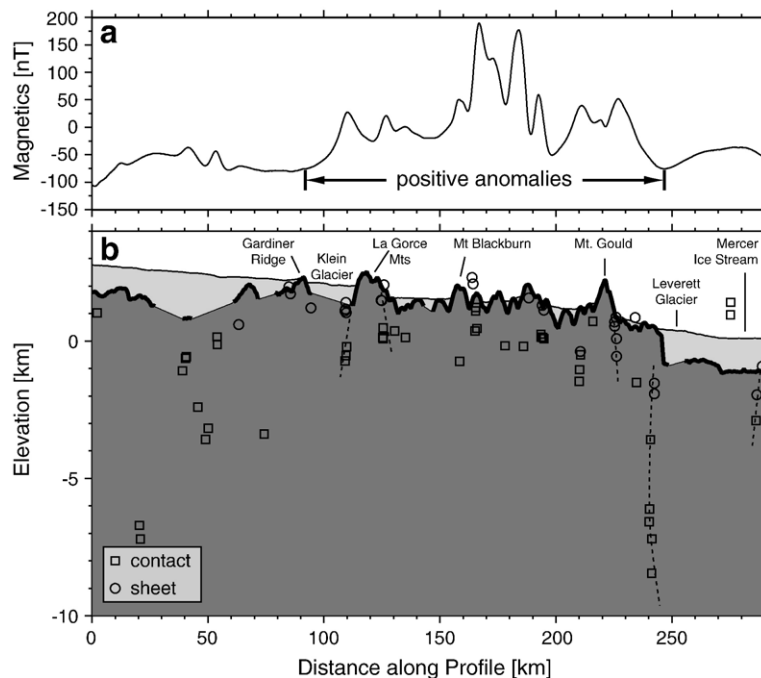


Fig. 7. Depth to magnetic source estimates using multiple-source Werner deconvolution. For location of profile see Fig. 2.

(km 550 to 720 in Figs. 4c and 6) and higher amplitudes. The profile view (Fig. 4c) illustrates wavelengths of several tens of kilometers with peak-to-trough amplitudes of more than 300 nT. In the area spanning the La Gorce Mtns, Mt. Blackburn and the Leverett Glacier, between 86°45'S and 85°30'S, positive anomalies have wavelengths of several tens of kilometers (Fig. 6). Two inferred faults from Katz [19], on the basis of morphologic and geologic constraints, that define the lateral extent of the Leverett Glacier, are paralleled by steep magnetic gradients in the western half of the survey area (white lines, Fig. 6). Between the Watson Escarpment and the Reedy Glacier, the magnetic field is dominated by positive amplitudes with wavelengths of several tens of kilometers. The magnetic field south of the area where rock outcrops are present is largely subdued with two exceptions (Fig. 6). A positive magnetic anomaly between 87°30'S and 87°S near 130°W trends approximately 160° (70°W), parallel to the steep magnetic gradient that borders the Leverett Glacier and the Mercer Ice Stream (Fig. 6). Between 150°W and 155°W a second circular shaped positive anomaly near the known rock outcrops of Mt. Howe, punctuates the magnetic lows that characterize the inland flank of the Transantarctic Mountains reflecting the non-magnetic character of the meta-sedimentary and meta-volcanic rocks of the region (Fig. 2).

The magnetic field over Mercer Ice Stream, north of 85°S, exhibits long-wavelength (>50 km) high-amplitude (>200 nT peak-to-trough) magnetic lows (Fig. 5d and km 720–820 in Fig. 4c). These magnetic anomalies could be caused by magnetic basement covered with thick sedimentary sequences or other sources of deep crustal magnetization (induced and remanent).

4.3. Gravity

As the free-air anomaly (Fig. 5e) largely reflects the subglacial topography (Fig. 5c) we will focus on the description of the Bouguer anomaly (Fig. 5f) because of its relevance for geologic and tectonic interpretation. We focus on the long wavelength structure of the Bouguer anomaly because it mostly reflects lateral changes in crustal thickness. Note that the data gaps in the bedrock topography and the free-air anomaly have been interpolated for the calculation of the Bouguer anomaly to aid map interpretation.

In the South Pole region, the gravity field is very smooth with a linear decrease in the Bouguer anomaly towards the Transantarctic Mountains (Fig. 4c) and little structure is discernible. One exception is a weak wedge-shaped gravity low near South Pole (Fig. 5f), trending about 160° (20°W). This Bouguer gravity low is slightly oblique to the magnetic anomaly near South Pole and

does not have a corresponding topographic structure. The Bouguer gravity minima occur about 150 km inland of the Transantarctic Mountains front (Figs. 4c and 5f) and correlate with regions of high elevation in the sub-ice bedrock topography. Within this regional low, a 20 to 40-km-wide linear low near 86°30'S is aligned at a slightly oblique angle to the front of the Transantarctic Mountains (Fig. 5f). This low defines a slight rotation in the trend of the primary structures compared to the mountain front. Along 85°45'S, a steep gradient in Bouguer gravity parallels the topographic expression of the Transantarctic Mountains (km 725 in Fig. 4). This gradient towards negative values marks the transition from the thin crust in the Ross Embayment to the thicker crust beneath the Transantarctic Mountains. The Bouguer anomaly over the Ross Embayment and the Mercer Ice Stream is smooth with positive amplitudes between 0 and 60 mGal (Figs. 4b and 5f).

4.4. Depth to magnetic source estimates

The estimated depth to the magnetic source is an important parameter that aids geologic and tectonic interpretation of observed magnetic anomalies. We use a multiple-source Werner deconvolution algorithm developed by Hansen and Simmonds [31] and implemented by Phillips [32] to estimate the depth to magnetic sources along individual profiles in the area with known geology from rock outcrops. Werner deconvolution has been used successfully for reconnaissance aerogeophysical surveys in Antarctica [10,33] and compared

successfully with seismic results [34]. For the data set discussed here, we found that 3 solutions per data window, a clustering radius of 5% of the depth of the solutions, and a minimum of 2 solutions per cluster produce reliable results. The criteria for evaluating the reliability of the solutions was to minimize the number of faulty depth solutions located above the bedrock/ice contact. These solutions can be created by noise in the data or interference of multiple anomalies within a data window and do not reflect magnetic sources. Because the nature of the magnetic sources is unknown, we have included both sheet and contact solutions in our analysis. Fig. 7 shows the depth estimates along a 300-km-long profile (see Fig. 2 for location). Along the profile, the depth to the magnetic sources often coincides with the elevation of the subglacial topography or rock outcrops. The sources of the positive magnetic anomalies between km 100 and 245 in Fig. 7 are very shallow with several clusters of depth solutions located between 1 and 2 km beneath the bedrock topography. There are several depth solutions that show long vertical clusters (dashed lines in Fig. 7) that are indicative of faulting or contacts and in most other cases we interpret the clusters of depth solutions as being related to the mapped and inferred faults. The magnetic anomalies related to these faults are likely caused by contrasts in magnetic susceptibility, and therefore lithology, across these faults.

The cluster north of Klein Glacier and south of the La Gorce Mtns (km 110 in Fig. 7) coincides with the location of mapped faults (Fig. 2). The northern flank of

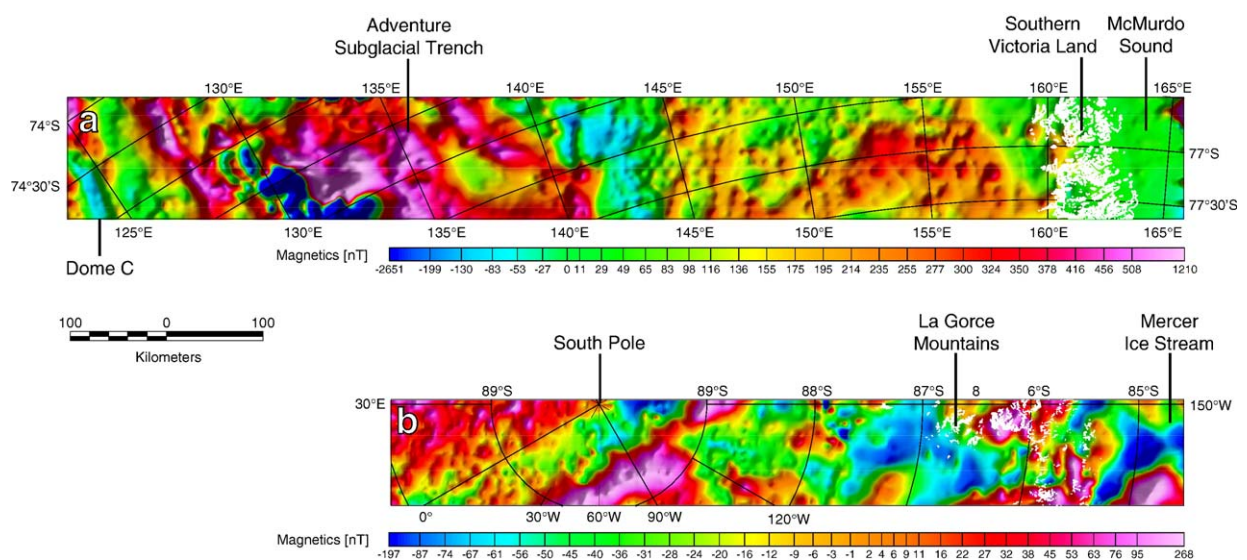


Fig. 8. a) Magnetic anomaly of the southern Victoria Land transect [10] and b) for the South Pole–Mercer Ice Stream transect. For location of both transects see Fig. 1. Both data sets have been draped to a surface 3.6 km above the bedrock topography. White areas indicate rock outcrops.

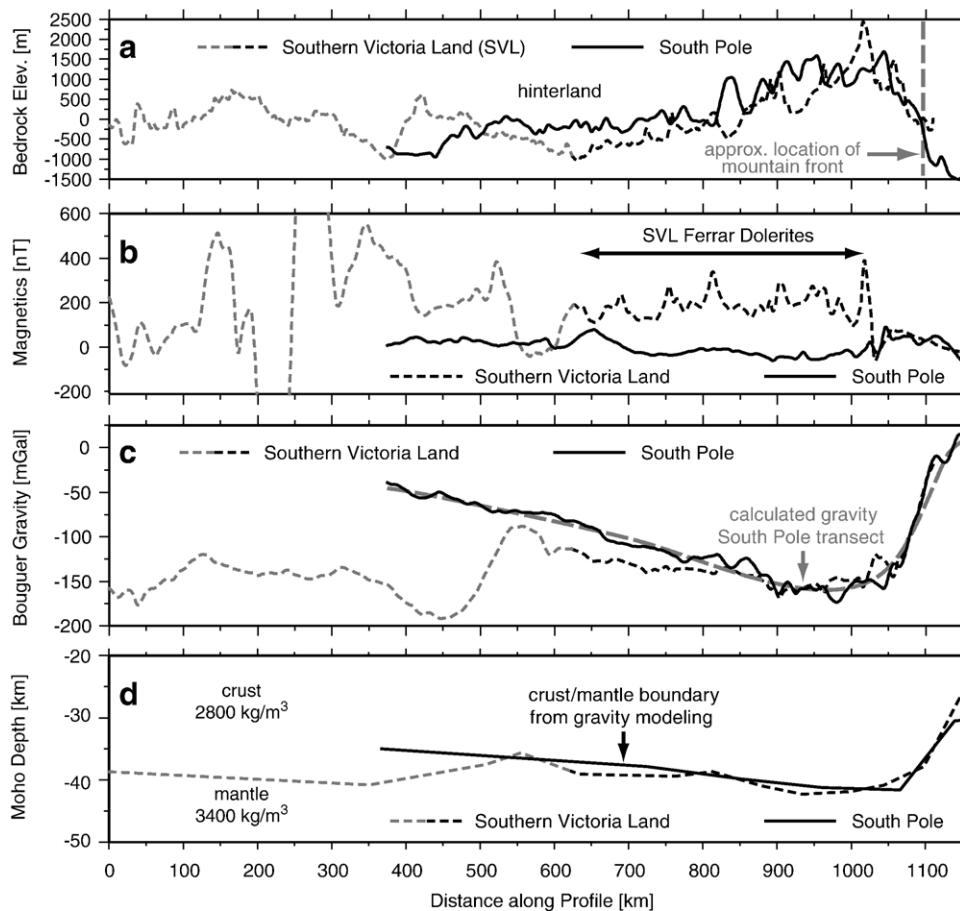


Fig. 9. Comparison between magnetic and Bouguer anomalies along the southern Victoria Land transect (dashed lines) and South Pole–Mercer Ice Stream (solid lines). The grey dashed portions of the southern Victoria Land transect mark regions that are tectonically different from the Transantarctic Mountains and are only shown for completeness. The comparison between the two transects is only discussed between km 625 and 1150. The profiles have been aligned horizontally at the approximate location of the mountain front. Grey long-dashed line in c) is calculated gravity from crustal structure in d). The southern Victoria Land crustal structure is from [10].

the La Gorce Mtns (km 125 in Fig. 7) is bounded by a vertical cluster of depth solutions that also coincides with the location of a mapped fault (Fig. 2). North of Mt. Gould and south of Leverett Glacier, two vertical streaks of solutions (km 225 and 245) are near the proposed major fault south of the Leverett Glacier (Fig. 2, [19]). The long wavelength of the magnetic anomaly (Fig. 7) supports a deep source of this anomaly as indicated by the vertical clustering of the depth solutions. The vertical streak of depth solutions coincides with a fault proposed by Katz [19] that runs along the northern boundary of the Wisconsin Range batholith in the western part of the survey area. However, this fault is not related to the edge of the batholith along its entire length because the continuation of this fault to the east, does not define the edge of the batholith since rocks of the Wisconsin Range batholith also crop out in the

Harold Byrd Mountains north of the Leverett Glacier (Fig. 2). Although the vertical streak of depth solutions coincides with Katz's [19] inferred fault it is more likely that the depth solutions reflect the northern boundary of the Wisconsin Range batholith in this case.

5. Interpretation and discussion

5.1. Magnetism

Observations from our magnetic survey strengthen the understanding of the geology on the inland flank of the Transantarctic Mountains. When compared to the geophysical transect across the Transantarctic Mountains in southern Victoria Land, the observed magnetic pattern over the South Pole–Mercer Ice Stream shows notable differences (Figs. 8, 9). Direct comparison of the

two data sets is made possible by draping the data onto a surface 3.6 km above the bedrock using Cordell's method [35]. The southern Victoria Land transect [10] exhibits short-wavelength magnetic anomalies, together with a terraced morphology in the ice-penetrating radar data, interpreted as sills of Jurassic Ferrar Dolerite overlying Beacon Supergroup strata [10]. A similar pattern of magnetic anomalies exists throughout Wilkes Land and elsewhere [30]. The absence of the typical magnetic pattern of Ferrar Dolerite sills in the South Pole–Mercer Ice Stream transect (Figs. 8 and 9) is consistent with the apparent lack of mesa landscape in the sub-ice topography. We interpret the lack of these diagnostic structures in both data sets as absence of Ferrar Dolerite sills within our survey area; noting that, due to the large flight line spacing of 10 km it is possible that Ferrar Dolerite was undetected between our survey lines. The only documented occurrence of Ferrar magmatism in the vicinity of our actual survey area is near the head of the Scott Glacier at Mt. Weaver [36,37] and at Mt. Griffith [21] both outside our survey area (Fig. 2). To date, there is no other Jurassic Ferrar magmatism documented in geologic maps of the survey area, consistent with our interpretation. The Ferrar large igneous province forms a 3500-km-long linear semi-continuous belt along the Transantarctic Mountains [38]. Along this belt, Ferrar Dolerite sills have been emplaced in several nodes where the cumulative thickness of the intrusions is greatest (up to 2 km). Between these centers of magma emplacement, the total thickness of the intruded rocks is greatly reduced or even nonexistent [e.g., 37 and references therein]. The closest magma nodes to our survey area are the Dufek intrusion in the Weddell Sea sector (700 km away) and in the Beardmore Glacier region (500 km away) (Fig. 1). The known thickness of the Beacon sediments within our survey area is only of the order of a few hundreds of meters [19,39], much thinner than the 2–2.5 km in southern Victoria Land [40]. Triassic strata are not present south of the Nielsen Plateau [38] and within our survey area. While thick sequences (~ 1 km) of dolerite are elsewhere intruded into Beacon sediments as little as 500 m thick [e.g., 37 and references therein], the absence of typical magnetic anomalies, mesa landscape, and known rock outcrops rules out a widespread presence of Ferrar Dolerite within our survey area.

The apparent total lack of Ferrar Dolerite in the survey area raises questions about the source of the magnetic anomalies. Stump et al. [41] and Doumani and Minshew [36] report Early Miocene McMurdo volcanics at Sheridan Bluff and Mount Early, at the head of the Scott Glacier near Mt. Weaver (Fig. 6). This is an unusual

occurrence for McMurdo volcanics as these rocks typically occur on the outboard side of the Transantarctic Mountains, near the coast. There are no other known occurrences of McMurdo volcanics within our actual survey area and the ice covered inland flank of the Transantarctic Mountains is dominated by a smooth negative magnetic field (Fig. 6) making a sub-ice presence unlikely. Therefore, Miocene McMurdo volcanics are unlikely to play a significant role in the observed magnetic field in the Scott and Reedy Glaciers area.

Other potential sources for the magnetic anomalies are the prevalent rocks of the Wisconsin Range and Queen Maud batholiths [17] part of the Cambro-Ordovician Granite Harbour Intrusive Complex [42]. Magnetic susceptibilities of the Wisconsin Range and Queen Maud batholith rocks are unknown; however, within Victoria Land the Granite Harbour Intrusives show a bimodal distribution [43]. Low magnetic susceptibilities are related to peraluminous phases that show no magnetic anomalies [44]. The “magnetite type” intrusive phases [43–45] exhibit positive anomalies with amplitudes of tens to hundreds of nT and widths of several tens of kilometers [44]. Over the Miller Range, the Granite Harbour Intrusive magnetic signature is negative, likely due to reversely magnetized intrusives or unusually non-magnetic basement [46] (C. Finn, pers. comm., 2006). The positive magnetic anomalies observed between the Scott and Reedy Glacier region resemble those observed over the Granite Harbour Intrusives in southern Victoria Land (Fig. 6), and they coincide with regions of known Granite Harbour Intrusives outcrops at the La Gorce Mtns, Mt. Blackburn, the Watson Escarpment and the Reedy Glacier (Fig. 6). These observations suggest that rocks of the Granite Harbour Intrusive suite are the likely source for the observed magnetic anomalies in the Scott and Reedy Glacier area. Our interpretation is based on the observation of similarities in magnetic anomalies over known occurrences of rocks of the Granite Harbour Intrusive suite in the Scott and Reedy Glacier area and Victoria Land and the assumption that these rocks have similar magnetizations in both regions. However, we cannot rule out changes in magnetization during tectonic or magmatic events following the emplacement of the Granite Harbour Intrusives. Volcanic rocks of the Wyatt Formation may contribute to the magnetic anomalies as well. However, hypabyssal intrusions are generally thin, which would result in much higher frequency and amplitude anomalies than observed. A closer correlation between lithology and magnetic anomalies will require new surveys with a closer flight line spacing and *in situ* measurements of magnetic susceptibilities.

A comparison of structural trends in the magnetic data on the inland flank of the Transantarctic Mountains (Fig. 8) from the two aerogeophysical transects reveals differences. In southern Victoria Land, the main structural trends are parallel to the Adventure Subglacial Trench and Resolution Subglacial Highlands (115°/25°W) at a 45° angle to the Transantarctic Mountains front (160°/0°) (Fig. 8a). The Resolution Subglacial Highlands mark the western extent of the magnetic Ferrar Dolerite signature, interpreted as the edge of the Neoproterozoic craton margin [10,23]. Furthermore, the known orientations at Vostok [33,47], the 90°E and Sovetskaya subglacial lakes within East Antarctica [48] are subparallel to the trends defined in southern Victoria Land and the Dome C area [10] (Fig. 1). In contrast, within the South Pole segment of the present survey, the dominant trend in the magnetic anomalies (180°/0°) is rotated 60° to the Transantarctic Mountains (120°/90°W) (Fig. 8b), at a high angle to the trend in southern Victoria Land. The contrasting trends are interpreted to most likely represent tectonic features of different origins.

The strength and linearity of the magnetic anomaly at South Pole triggers an obvious speculation about its continuation towards the Transantarctic Mountains. The magnetic lineament projects toward a linear fault, 250 km long, along 180° longitude between the South Pole and the Transantarctic Mountains (Fig. 1) interpreted from ice-penetrating radar data from reconnaissance flights (see Fig. 3 in [28]). If continued northward, the proposed fault [28] would intersect the Transantarctic Mountains in the region of the Shackleton Glacier (Fig. 1). This trend is also subparallel to the dominant orientation of faults within our survey area (Fig. 2), and parallels the tectonic trends in the Ross Sea, defined by the sedimentary basins (Fig. 1).

The Shackleton Glacier is recognized as a geologic boundary that separates contrasting basement age provinces of the central Transantarctic Mountains and the southern Transantarctic Mountains [49–51]. Sm–Nd isotope data from plutons show a distinct change in basement model ages from 2.2–1.6 Ga east of the Shackleton Glacier to 1.5–1.1 Ga west of the Shackleton Glacier (relative to the Prime Meridian). Furthermore, Early to Middle Cambrian volcanic rocks are abundant west of Shackleton Glacier, but sparse east of the Shackleton Glacier [52]. Contrasting apatite fission track data from either side indicate the presence of a major transverse fault, active in the Cenozoic [53]. There are no magnetic data over the Shackleton Glacier area to test the hypothesis that the magnetic lineament at South Pole is a subglacial expression of the same boundary. The coincidence of a documented geologic boundary [49–51], an interpreted fault delineated from

the subglacial topography [28], and the well-defined linear magnetic anomaly identified in this study (Fig. 5d) leads us to interpret a lithospheric-scale structure in this sector, at a high angle to the Transantarctic Mountains front. We propose the name “South Pole Lineament” for this feature in light of its location and parallelism with the Prime Meridian. We speculate that the subdued expression of the feature with respect to gravity and sub-ice topography beneath the South Pole itself may be attributed to sediment infill, consistent with the smooth, gradual Bouguer characteristics (Fig. 5f) and the absence of rough topography (Fig. 5d).

Further support for this interpretation potentially comes from seismic and magnetotelluric experiments near South Pole, which coincidentally were situated over or flanking the now-identified magnetic low (Fig. 5). The seismic experiment yielded no refracted arrivals from the bed-ice transition, interpreted as an indication that a layer of low velocity rocks overlies acoustic basement at South Pole [54,55]. Electrical resistivity data from a magnetotelluric survey [56] suggest the presence of at least 1 km of sediments beneath South Pole. Wannamaker et al. [56] suggest that this may represent an inland extension of the Beacon Supergroup; however, the characteristic mesa and terrace morphology to be expected is not evident in our sub-ice topography data. Our airborne gravity data are unable to detect such a thin layer of sediments.

Previous analyses of satellite magnetic data [23] and teleseismic tomography [57] predict that the edge of the undeformed East Antarctic craton corresponds to a magnetic gradient and a transition from high to low seismic velocities near South Pole, far inland from the exposed Transantarctic Mountains. The interpretation of satellite magnetic data correlates highs with the Precambrian shield basements and lows with magnetite-poor reworked craton-margin rocks [23]. Potentially, the observed aeromagnetic trend at South Pole corresponds to the edge of the East Antarctic craton, or a younger structure, such as an intracontinental transform localized along this inherited boundary.

5.2. Gravity

The Bouguer gravity anomaly of the South Pole–Mercer Ice Stream transect and the southern Victoria Land transect show strong similarities (Fig. 9c). Both transects show a steep gradient towards the Ross Sea side and a gentle gradient in the hinterland. The long wavelength Bouguer gravity anomaly largely reflects crustal structure related to lateral crustal thickness variations. For this reason and because of the strong similarities of the Bouguer gravity between the two

regions, the deep crustal and upper mantle structures of both regions are likely similar as well. We have modeled the crustal thickness along the South Pole–Mercer Ice Stream transect assuming that there are no lateral density changes (Fig. 9d). To compare this model to the southern Victoria Land transect we use the same crustal density of 2800 kg/m^3 and a mantle density of 3400 kg/m^3 [10]. The absolute thickness of the crust is unknown and for this reason we have used the same thickness under the mountain front as for the southern Victoria Land transect. The calculated gravity, using a slight crustal thickening of 5 km beneath the mountain range and a sharp crustal thickness reduction of ~ 10 km towards the Ross Ice Shelf, matches the observed Bouguer gravity (Fig. 9c). The grey dashed portions of the southern Victoria Land transect (Fig. 9d) mark regions that are tectonically different from the Transantarctic Mountains and are only shown for completeness. The comparison between the two transects is only discussed between km 625 and 1150. The modeled crustal structure along the South Pole–Mercer Ice Stream transect is very similar to southern Victoria Land (Fig. 9d). Overall, the shape of the sub-ice topography along the South Pole transect inland of the Transantarctic Mountains, as well as the Cenozoic faulting patterns in the Scott Glacier region [19,21] are not compatible with a flexural uplift model for the formation of the Transantarctic Mountains [e.g., 22]. Furthermore, the denudation pattern across the exposed Transantarctic Mountains (in the Scott Glacier region) along the South Pole transect does not follow an exponential trend that would be expected from a broken plate model [21]. We note that in other places along the Transantarctic Mountains, the structure of the Kukri Peneplain does not follow a simple exponential decay either. For example, in the Beardmore and Nimrod Glacier area, Barrett et al. [58] and Fitzgerald et al. [59] report a broad syncline in the structure of the Kukri Peneplain that is difficult to explain by flexural unloading of a broken plate. If a common mechanism such as flexural unloading of a broken plate was responsible for the uplift and formation of the Transantarctic Mountains we would expect to see commonalities in structure and denudation patterns between the two aerogeophysical transects. That we do not, suggests that modification, or re-evaluation of the broken plate model is required.

6. Conclusions

More than 13,000 line-km of aerogeophysical data have been used to compile gravity, magnetic and

subglacial topography maps of an area 810×100 km wide between South Pole and Mercer Ice Stream. The main results are:

- 1) In contrast to the magnetic data, the gravity data in the South Pole–Mercer Ice Stream transect is very similar to the southern Victoria Land transect. Forward modeling of the gravity data suggests slight crustal thickening of 5 km beneath the mountain front, similar to southern Victoria Land.
- 2) The subglacial morphology within the survey area can be divided into four distinct provinces: a low lying region beneath South Pole with smooth topography and generally bright bed reflections, a region with deeply incised U-shaped valleys on the inland flank of the Transantarctic Mountains, the Transantarctic Mountains with exposed rock outcrops, and the low lying region beneath Mercer Ice Stream and the Ross Ice Shelf. The typical mesa landscape, observed in southern Victoria Land and elsewhere along the Transantarctic Mountains was not recognized within our survey area.
- 3) The typical pattern of short-wavelength and high amplitude anomalies caused by the Jurassic tholeiitic magmatism in the form of dolerite sills and basaltic flows along the Transantarctic Mountains is not observed. This is consistent with the subglacial morphology observed in ice-penetrating radar data that does not reveal the typical mesa landscape within the survey area and the lack of Ferrar Dolerite sills observed in geological field mapping. Together these observations rule out a widespread presence of Jurassic magmatism between the Scott and Reedy Glaciers.
- 4) Over the Transantarctic Mountains, the magnetic anomaly field shows several small (tens of kilometers) positive amplitudes that can be correlated with known rock outcrops of Granite Harbour Intrusives. The observed anomaly pattern is similar to the magnetic field over the Granite Harbour Intrusives in Victoria Land. Source depth estimates, using multiple-source Werner deconvolution, indicate shallow sources for the Granite Harbour Intrusives that dominate the observed magnetic field over the Transantarctic Mountains.
- 5) Several geologic contacts, often fault related, were mapped by multiple-source Werner deconvolution of the magnetic data.
- 6) A pronounced magnetic lineament (herein named the South Pole Lineament) can be recognized beneath the South Pole that defines for the first time the tectonic fabric of the region. The orientation of this structure

coincides with a proposed fault interpreted from ice-penetrating radar data [28] and a major boundary in Proterozoic basement Sm–Nd model ages across the Shackleton Glacier [49]. The orientation of these structural trends is very different from the southern Victoria Land transect and trends observed elsewhere in the East Antarctic craton. The South Pole Lineament likely reflects a previously unknown major tectonic trend of the East Antarctic craton related to formation or disintegration of Rodinia and Gondwana supercontinents or the edge of the craton.

Acquisition of aerogeophysical transects over the exposed Transantarctic Mountains and reaching deep into the interior of the ice-covered East Antarctic shield is a powerful tool for advancing our understanding of the margin of the shield and its relation to younger tectonic events. Future aerogeophysical surveys will help to further constrain the structure and composition of the East Antarctic shield.

Acknowledgements

We thank the National Science Foundation's SOAR facility for data acquisition, support, and reduction of the ice-penetrating radar data. Robert Arko (LDEO) is thanked for reducing the GPS, gravity, and magnetic data. Christine Siddoway is thanked for numerous stimulating discussions during her research leave at Lamont and for her many suggestions that improved the paper. Thoughtful comments and suggestions by Carol Finn and an anonymous reviewer helped clarify and improve this paper. Funding was provided by the National Science Foundation (OPP 96-15704 and 03-38281 to LDEO, and OPP 96-15294 and 03-38009 to Syracuse University). LDEO contribution 6948.

References

- [1] I.W.D. Dalziel, D.H. Elliot, West Antarctica; problem child of Gondwanaland, *Tectonics* 1 (1982) 3–19.
- [2] J.W. Goodge, From Rodinia to Gondwana: supercontinent evolution in the Transantarctic Mountains, in: J.A. Gamble, D.N.B. Skinner, S. Henrys (Eds.), *Antarctica at the Close of a Millennium*, Royal Society of New Zealand Bulletin, vol. 35, The Royal Society of New Zealand, Wellington, New Zealand, 2002, pp. 61–74.
- [3] G. Capponi, B. Messiga, G.B. Piccardo, M. Scambelluri, G. Traverso, R. Vannucci, Metamorphic assemblages in layered amphibolites and micaschists from the Dessent Formation (Mountaineer Range, Antarctica), *Mem. Soc. Geol. Ital.* 43 (1990) 87–95.
- [4] D.L. Schmidt, P.D. Rowley, Continental rifting and transform faulting along the Jurassic Transantarctic Rift, Antarctica, *Tectonics* 5 (1986) 279–291.
- [5] D.H. Elliot, Jurassic magmatism and tectonism associated with Gondwanaland break-up; an Antarctic perspective, in: B.C. Storey, T. Alabaster, R.J. Pankhurst (Eds.), *Magmatism and the Causes of Continental Breakup*, Geological Society Special Publications, vol. 68, Geological Society of London, London, United Kingdom, 1992, pp. 165–184.
- [6] T.J. Wilson, Jurassic faulting and magmatism in the Transantarctic Mountains; implications for Gondwana breakup, in: R.H. Findlay, R. Unrug, M.R. Banks, J.J. Veevers (Eds.), *Assembly, Evolution and Dispersal; Proceedings of the Gondwana Eight Symposium*, International Gondwana Symposium 8, International Gondwana Symposium, 1993, pp. 563–572.
- [7] P.G. Fitzgerald, Tectonics and landscape evolution of the Antarctic plate since the breakup of Gondwana, with an emphasis on the West Antarctic Rift System and the Transantarctic Mountains, in: J.A. Gamble, D.N.B. Skinner, S.A. Henrys (Eds.), *Antarctica at the Close of a Millennium*, Royal Society of New Zealand Bulletin, vol. 35, The Royal Society of New Zealand, Wellington, New Zealand, 2002, pp. 453–469.
- [8] P.J. Barrett, Antarctic palaeoenvironment through Cenozoic times; a review, *Terra Antarctica* 3 (1996) 103–119.
- [9] Cape Roberts Science Team, Studies from the Cape Roberts Project; Ross Sea, Antarctica, initial report on CRP-3, *Terra Antarctica* 7 (1/2) (2000) 185–209.
- [10] M. Studinger, R.E. Bell, W.R. Buck, G.D. Karner, D.D. Blankenship, Sub-ice geology inland of the Transantarctic Mountains in light of new aerogeophysical data, *Earth Planet. Sci. Lett.* 220 (2004) 391–408.
- [11] E. Stump, *The Ross Orogen of the Transantarctic Mountains*, Cambridge University Press, New York, NY, United States, 1995 284 pp.
- [12] V.H.J. Minshew, Geology of the Scott Glacier and Wisconsin Range areas, central Transantarctic Mountains, Antarctica, Doctoral Thesis, Ohio State University, 1967.
- [13] E. Stump, Stratigraphy of the Ross Supergroup, central Transantarctic Mountains, *Antarct. Res. Ser.* 36 (1985) 225–274.
- [14] E. Stump, Type locality of the Ackerman Formation, La Gorce Mountains, Antarctica, in: R.L. Oliver, P.R. James, J.B. Jago (Eds.), *Antarctic Earth Science; Fourth International Symposium*, Cambridge Univ, Cambridge, United Kingdom, 1983, pp. 170–174.
- [15] A.J. Rowell, D.A. Gonzales, L.W. McKenna, K.R. Evans, E. Stump, S.W.R. Van, Lower Paleozoic rocks in the Queen Maud Mountains, revised ages and significance, in: C.A. Ricci (Ed.), *The Antarctic Region: Geological Evolution and Processes; Proceedings of the VII International Symposium on Antarctic Earth Sciences*, International Symposium on Antarctic Earth Sciences, vol. 7, Terra Antarctica Publication, Siena, Italy, 1997, pp. 201–207.
- [16] J.G. Murtaugh, Geology of the Wisconsin Range batholith, Transantarctic Mountains, N.Z. J. Geol. Geophys. 12 (1969) 526–550.
- [17] S.G. Borg, Petrology and geochemistry of the Queen Maud Batholith, central Transantarctic Mountains, with implications for the Ross Orogeny, in: R.L. Oliver, P.R. James, J.B. Jago (Eds.), *Antarctic Earth Science; Fourth International Symposium*, Cambridge Univ, Cambridge, United Kingdom, 1983, pp. 165–169.
- [18] J.P. Encarnacion, A.M. Grunow, Changing magmatic and tectonic styles along the paleo-Pacific margin of Gondwana and the onset of Early Paleozoic magmatism in Antarctica, *Tectonics* 15 (1996) 1325–1341.
- [19] H.R. Katz, Post-Beacon tectonics in the region of Amundsen and Scott Glaciers, Queen Maud Range, Transantarctic Mountains, in: C. Craddock (Ed.), *Antarctic Geoscience*, International

- Union of Geological Sciences. Series B, vol. 4, International Union of Geological Sciences (IUGS), Oslo, International, 1982, pp. 827–834.
- [20] C. Siddoway, M.F. Siddoway, Addressing the longitudinal reference problem in Antarctica: a method for regional comparison of structural data using modular arithmetic, *Terra Antart. Rep.* 12 (2006) 119–132.
- [21] P.G. Fitzgerald, E. Stump, Cretaceous and Cenozoic episodic denudation of the Transantarctic Mountains, Antarctica: new constraints from apatite fission track thermochronology in the Scott Glacier region, *J. Geophys. Res., [Solid Earth]* 102 (1997) 7747–7765.
- [22] U.S. ten Brink, R.I. Hackney, S. Bannister, T.A. Stern, Y. Makovsky, Uplift of the Transantarctic Mountains and the bedrock beneath the East Antarctic ice sheet, *J. Geophys. Res., [Solid Earth]* 102 (1997) 27603–27621.
- [23] C.A. Finn, J.M. Goodge, D. Damaske, C.M. Fanning, Scouting craton's edge in Paleo-Pacific Gondwana, in: D.K. Fütterer, D. Damaske, G. Kleinschmidt, H. Miller, F. Tessensohn (Eds.), *Antarctica: Contributions to Global Earth Sciences*, Springer-Verlag, Berlin, 2006, pp. 165–174.
- [24] G.L. Mader, Dynamic positioning using GPS carrier phase measurements, *Manuscr. Geod.* 11 (1986) 272–277.
- [25] D.D. Blankenship, D.L. Morse, C.A. Finn, R.E. Bell, M.E. Peters, S. D. Kempf, S.M. Hodge, M. Studinger, J.C. Behrendt, J.M. Brozena, Geologic controls on the initiation of rapid basal motion for the ice streams of the Southeastern Ross Embayment; a geophysical perspective including new airborne radar sounding and laser altimetry results, *Antart. Res. Ser. West Antarctic Ice Sheet Behav. Environ.* 77 (2001) 105–122.
- [26] R.E. Bell, V.A. Childers, R.A. Arko, D.D. Blankenship, J.M. Brozena, Airborne gravity and precise positioning for geologic applications, *J. Geophys. Res.* 104 (1999) 15281–15292.
- [27] V.A. Childers, R.E. Bell, J.M. Brozena, Airborne gravimetry; an investigation of filtering, *Geophysics* 64 (1999) 61–69.
- [28] D.J. Drewry, Subglacial morphology between the Transantarctic Mountains and the South Pole, *Antarctic Geology and Geophysics*, International Union of Geological Sciences. Series B, vol. 1, International Union of Geological Sciences (IUGS), Oslo, International, 1972, pp. 693–703.
- [29] M.B. Davis, Subglacial morphology and structural geology in the Southern Transantarctic Mountains from airborne geophysics, M.S. thesis, The University of Texas, 2001.
- [30] R.H.N. Steed, Structural interpretations of Wilkes Land, Antarctica, in: R.L. Oliver, P.R. James, J.B. Jago (Eds.), *Antarctic Earth Science: Fourth International Symposium*, Cambridge Univ, Cambridge, United Kingdom, 1983, pp. 567–572.
- [31] R.O. Hansen, M. Simmonds, Multiple-source Werner deconvolution, *Geophysics* 58 (1993) 1792–1800.
- [32] J.D. Phillips, Potential-Field Geophysical Software for the PC, version 2.2, U. S. Geological Survey, Reston, VA, United States, 1997 34 pp.
- [33] M. Studinger, G.D. Karner, R.E. Bell, V. Levin, C.A. Raymond, A.A. Tikku, Geophysical models for the tectonic framework of the Lake Vostok region, East Antarctica, *Earth Planet. Sci. Lett.* 216 (2003) 663–677.
- [34] G.D. Karner, M. Studinger, R.E. Bell, Gravity anomalies of sedimentary basins and their mechanical implications: application to the Ross Sea basins, West Antarctica, *Earth Planet. Sci. Lett.* 235 (2005) 577–596.
- [35] L.E. Cordell, Techniques, applications, and problems of analytical continuation of New Mexico aeromagnetic data between arbitrary surfaces of very high relief, *Proceedings of the International Meeting on Potential Fields in Rugged Topography*, Bulletin, vol. 7, Institute of Geophysics, University of Lausanne, Switzerland, 1985, pp. 96–99.
- [36] G.A. Doumani, V.H. Minshew, General geology of the Mount Weaver area, Queen Maud Mountains, Antarctica, *Antart. Res. Ser.* 1299 (1965) 127–139.
- [37] D.H. Elliot, T.H. Fleming, Occurrence and dispersal of magmas in the Jurassic Ferrar large igneous province, Antarctica, *Gondwana Res.* 7 (1) (2004) 223–237.
- [38] D.H. Elliot, Jurassic magmatism and tectonism associated with Gondwanaland break-up; an Antarctic perspective, in: B.C. Storey, T. Alabaster, R.J. Pankhurst (Eds.), *Magmatism and the Causes of Continental Break-Up*, Geological Society Special Publications, vol. 68, Geological Society of London, London, United Kingdom, 1992, pp. 165–184.
- [39] A. Mirsky, Geology of the Ohio Range–Liv Glacier Area, Map Folio Series, folio 12, plate XVI, *Am. Geogr. Soc.*, New York, 1969.
- [40] P.J. Barrett, The Devonian to Triassic Beacon Supergroup of the Transantarctic Mountains and correlatives in other parts of Antarctica, in: R.J. Tingey (Ed.), *The Geology of Antarctica*, Oxford Monographs on Geology and Geophysics, vol. 17, Oxford University Press, Oxford, United Kingdom, 1991, pp. 120–152.
- [41] E. Stump, M.F. Sheridan, S.G. Borg, J.F. Sutter, Early Miocene subglacial basalts, the East Antarctic ice-sheet, and uplift of the Transantarctic Mountains, *Science* 207 (1980) 757–759.
- [42] B.M. Gunn, G. Warren, Geology of Victoria Land Between the Mawson and Mulock Glaciers, Antarctica, New Zealand Geological Survey, Wellington, New Zealand, 1962 157 pp.
- [43] E. Bozzo, A. Colla, A. Meloni, Ground magnetics in north Victoria Land (East Antarctica), in: Y. Yoshida, K. Kaminuma, K. Shiraishi (Eds.), *Recent Progress in Antarctic Earth Science*, Terra Sci, Tokyo, 1992, pp. 563–569.
- [44] F. Ferraccioli, E. Bozzo, Inherited crustal features and tectonic blocks of the Transantarctic Mountains; an aeromagnetic perspective (Victoria Land, Antarctica), *J. Geophys. Res. B, Solid Earth Planets* 104 (1999) 25,297–225,319.
- [45] R. Biagini, G. Di Vincenzo, C. Ghezzo, Petrology and geochemistry of peraluminous granitoids from Priestley and Aviator Glacier region, northern Victoria Land, Antarctica, *Mem. Soc. Geol. Ital.* 46 (1991) 205–230.
- [46] J.M. Goodge, C.A. Finn, D. Damaske, J. Abraham, H. Moeller, E. Anderson, N. Roland, F. Goldmann, P. Braddock, M. Rieser, Aeromagnetic and gravity data reveal crustal structure and tectonic history of the central Transantarctic Mountains region, *Eos Trans. AGU* 85 (47) (2004) (Fall Meet. Suppl., Abstract T11A-1237).
- [47] M. Studinger, R.E. Bell, G.D. Karner, A.A. Tikku, J.W. Holt, D.L. Morse, T.G. Richter, S.D. Kempf, M.E. Peters, D.D. Blankenship, R.E. Sweeney, V.L. Rystrom, Ice cover, landscape setting, and geological framework of Lake Vostok, East Antarctica, *Earth Planet. Sci. Lett.* 205 (2003) 195–210.
- [48] R.E. Bell, M. Studinger, M. Fahnestock, C.A. Shuman, Tectonically controlled subglacial lakes on the flanks of the Gamburtsev subglacial mountains, East Antarctica, *Geophys. Res. Lett.* 33 (2006) L02504.
- [49] S.G. Borg, D.J. DePaolo, B.M. Smith, Isotopic structure and tectonics of the central Transantarctic Mountains, *J. Geophys. Res., [Solid Earth Planets]* 95 (1990) 6647–6667.
- [50] S.G. Borg, D.J. DePaolo, A tectonic model of the Antarctic Gondwana margin with implications for southeastern Australia —

- isotopic and geochemical evidence, *Tectonophysics* 196 (1991) 339–358.
- [51] S.G. Borg, D.J. DePaolo, Laurentia, Australia, and Antarctica as a Late Proterozoic supercontinent — constraints from isotopic mapping, *Geology* 22 (1994) 307–310.
- [52] E. Stump, The Ross Orogen of the Transantarctic Mountains in light of the Laurentia–Gondwana split, *GSA Today* 2 (1992) 1–31.
- [53] P.G. Fitzgerald, S.L. Baldwin, S.R. Miller, P.B. O’Sullivan, Episodic Cenozoic Denudation in the Shackleton Glacier Area of the Transantarctic Mountains: a Record of Changing Stress Regimes? Ninth International Symposium on Antarctic Earth Sciences, Potsdam, Germany, 2003.
- [54] C.R. Bentley, J.W. Clough, Antarctic subglacial structure from seismic refraction measurements, *Antarctic Geology and Geophysics*, International Union of Geological Sciences. Series B, vol. 1, International Union of Geological Sciences (IUGS), Oslo, International, 1972, pp. 683–691.
- [55] E.S. Robinson, Some aspects of subglacial geology and glacial mechanics between South Pole and the Horlick Mountains, *Res. Rep. Ser., Dep. Geol., Geophys. & Polar Res. Center, Univ. Wis.*, 1964 88 pp.
- [56] P.E. Wannamaker, J.A. Stodt, L. Pellerin, S.L. Olsen, D.B. Hall, Structure and thermal regime beneath the South Pole region, East Antarctica, from magnetotelluric measurements, *Geophys. J. Int.* 157 (2004) 36–54.
- [57] M.H. Ritzwoller, N.M. Shapiro, A.L. Levshin, G.M. Leahy, Crustal and upper mantle structure beneath Antarctica and surrounding oceans, *J. Geophys. Res. B, Solid Earth Planets* 106 (2001) 30,645–630,670.
- [58] P.J. Barrett, J.F. Lindsay, J. Gunner, Reconnaissance geologic map of the Mount Rabot Quadrangle, Transantarctic Mountains, scale 1:250,000 U.S. Geological Survey, Reston, VA, 1970.
- [59] P.G. Fitzgerald, Thermochronologic constraints on post-Paleozoic tectonic evolution of the central Transantarctic Mountains, *Tectonics* 13 (1994) 818–836.
- [60] M.B. Lythe, D.G. Vaughan, BEDMAP-Consortium, BEDMAP-Bed Topography of the Antarctic, British Antarctic Survey, Cambridge, 2000.
- [61] M.B. Davis, D. Blankenship, *Geology of the Scott-Reedy Glaciers Area, Southern Transantarctic Mountains, Antarctica*, GSA Map Series MCH093F, The Geological Society of America, Boulder, CO, 2005.
- [62] K. Jezek, RAMP Product Team, RAMP AMM-1 SAR Image Mosaic of Antarctica, Fairbanks, AK: Alaska SAR Facility, in Association with the National Snow and Ice Data Center, Boulder, CO, Digit. Media (2002) (<http://www.nsidc.org/data/nsidc-0082.html>).